SECOND-ORDER COHERENCE MEASUREMENT OF SCATTERED LIGHT BY BROWNIAN PARTICLE

by

MINGZE QING
(B.S., Sichuan University)

A THESIS SUBMITTED FOR THE DEGREE OF

MASTER OF SCIENCE BY RESEARCH

in

PHYSICS DEPARTMENT

in the

GRADUATE DIVISION

of the

NATIONAL UNIVERSITY OF SINGAPORE

2024

Supervisor:
Professor Christian Kurtsiefer

Examiners:

Declaration

I hereby declare that this thesis is my original work and it has been written by me in its entirety. I have duly acknowledged all the sources of information which have been used in the thesis.

This thesis has also not been submitted for any degree in any university previously.

Mingze Qing

15 October 2019

Acknowledgments

Contents

Abstract

Second-order coherence measurement of scattered light by Brownian particle

by

Mingze Qing

MASTER OF SCIENCE BY RESEARCH in PHYSICS DEPARTMENT

National University of Singapore

Dynamic light scattering (DLS) is a technique that is widely used to determine the size distribution profile of Brownian particles in suspension or polymers in solution in many fields. In contrast, if the conditions of the solution were designed, the coherent properties of the scattered light could be studied by measuring the photon correlation function in the DLS technique. In this thesis, We will measure the classical second-order coherence function of scattered light and the interferometric photon correlation function respectively. The former function demonstrates the basic coherent properties of scattered light. Based on DLS theory, we can reduce the coherence time of scattered light by changing experimental parameters. The latter function is a coherent experimental method that can be used to distinguish between thermal and pseudothermal light and separate the amplitude fluctuations from the center of the function plot. We will analyze the results obtained in the experiment and propose existing questions and the next steps for the experiment.

List of Figures

List of Tables

Chapter 1

Introduction

Ever since lasers came into being in the 1960s, the principles and usage of light scattering (LS) techniques have expanded into numerous domains of study. The inelastic traditional light scattering (ILS) methods, along with dynamic light scattering (DLS), have been used to probe an array of particles[1]. As experimental practices continue to progress, DLS has become the popular approach to the analysis of the size distribution of particles undergoing Brownian motion, typically those smaller than the wavelength of monochromatic light in suspensions, or polymers in a solution. In DLS experiments, the temporal modulation of light due to scattering is usually detected by intensity or photon autocorrelation function. Therefore, the coherence properties of scattered light can be further analyzed using this photon coherence technique, which is often called the second-order coherence function $g^{(2)}$.

With regard to the coherence properties of light, coherence measures the relationship among the phases noted at various parts of a wave, containing both the temporal and spatial dimensions. It denotes a scenario where two sources of waves are considered coherent if they possess the same frequencies and waveforms. As an ideal quality of waves that display uniform interference patterns, coherence elaborates the connection between physical properties within a particular wave or between groups of waves.

Temporal coherence assesses the phase correlation of a light wave at varied spots along its pathway, assisting in understanding the extent of monochromaticity demonstrated by the source. In contrast, the phase correlation of light waves at different points in the plane perpendicular to the direction of propagation can be analyzed by spatial coherence. Thus revealing the degree of consistency in the wavefront's phase[2]. Temporal and spatial coherence primarily differ in their areas

of concern: The correlation between different time waves in the same space can be analyzed by temporal coherence while the correlation between waves at different points in the same time, whether crossing or parallel in the same direction, can be analyzed by spatial coherence.

By studying coherence, properties of light can be obtained for various aspects: the size of the light source can be obtained by measuring the spatial interference patterns or the coherence time of light. By measuring coherence, it is possible to understand different emission processes of light, such as the thermal or chaotic emission of a light bulb or the stimulated emission of a laser. When studying the scattering of light by atoms or molecules or Brownian particles, coherence can be used to understand the interaction between light and matter and even to measure the properties of particles.

With the ongoing development of research on the temporal coherence of light, the proposed second-order temporal coherence function $g^{(2)}(\tau)$ has become a new research stage in the development of quantum optics [3]. For fields that display Gaussian process characteristics, particularly chaotic light, the coherence function $g^{(n)}(\tau)$ shows a distinct relationship. Specifically, for spatially coherent polarized chaotic light, there is a simple relationship between the magnitude of the second-order correlation function $g^{(2)}(\tau)$ and the first-order correlation function $g^{(1)}(\tau)$

$$g^{(2)}(\tau) = 1 + \beta|g^{(1)}(\tau)|^2 \tag{1.1}$$

This function was proposed by physicist Siegert, known as the Siegert relation [4]. An immediate implication is that light exhibits a significant intensity correlation at zero time difference, a phenomenon commonly known in historical documentation as the "photon bunching" or "Hanbury Brown and Twiss" effect, $g^{(2)}(0) > g^{(2)}(\tau \longrightarrow \infty) = 1$. The Siegert relation is commonly used in connection with the Wiener-Khintchine theorem, which deduces the correlation between the spectral line width of light and the correlation time of fluctuations in its intensity. In many fields like astronomy, biology, and dynamic light scattering [5], the relation between these two functions is widely utilized.

However, different from the ideal Siegert relation, a factor $\beta < 1$ can be added in the experiment due to the influence of the field or intensity of unrelated spots. Consider the reduction in contrast as an average. In the experiment, since the

scattered field is usually unpolarized, it can be regarded as the superposition of two independent speckle patterns and has a certain average intensity ratio of $P = \langle I_1 \rangle / \langle I_2 \rangle$. If we do not take into account the effect of spatial averages, for example, with a single-mode fiber, the summary of intensity consists of only two components, which provides a precise analysis of this phenomenon. Therefore, the coefficients of the second-order coherence function also change. [6]

$$\beta = \frac{1 + p^2}{(1 + p)^2} \tag{1.2}$$

Observations of photon bunching in light emitted from a chaotic source through beamsplitter experiments, conducted by Brown and Twiss[7] [8], sparked the advent of modern quantum optics. Furthermore, $g^{(2)}$ offers a beneficial method for distinguishing and categorizing the primary light types: thermal, coherent laser, and single photon light.

While a stable coherent wave can only achieve $g^{(2)}(0) = 1$, $g(0) > 1$ doesn't always imply the presence of incoherent chaotic light. This situation could also be attributed to a coherent quantum state with short amplitude fluctuations. For a laser light, the electric field can be represented by the Schawlow-Townes process illustrating phase diffusion. This process can be seen as short, sudden, and random shifts in the phase of the fluctuating coherent field. Under these jumps, the second-order coherence function of the laser always maintains a stable coherence and the value is a constant $g^{(2)}(0) = 1$ flats at 1. When the amplitude gain in the laser is not fixed, but changes periodically, it will cause fluctuations in the laser output intensity, resulting in $g^{(2)}(0) > 1$, and no chaotic light is introduced into the laser beam. Therefore, only based on the value of $g^{(2)}(0)$, it is insufficient to differentiate between chaotic and coherent light with amplitude modulation.

To solve this problem, Lebreton [9] proposes a theory around interferometric photon correlation experiments that use a non-equilibrium Michelson interferometer and introduce a time delay. The experiment shows that the interference cross-correlation function of chaotic light is obviously different from that of stable coherent light, so the unique identification mark of each light source is established. The experimental result also shows that this method can also distinguish chaotic light

from amplitude-modulated coherent light by interference correlation function which even have similar first and second-order correlation functions.

From the introduction of the cross-correlation function, this experimental method can be utilized to distinguish and explore the characteristics of thermal and pseudothermal light. For instance, pseudothermal light generated from microsphere scattering can be used in dynamic light scattering technique, as we mentioned before, the measurement is done for the particle size distribution of tiny particles in suspension or polymers in solution. The analysis of cross-correlation experimental results can extract information about the amplitude and phase fluctuations of scattered light, thereby providing a more in-depth analysis of the properties of such scattered light.

1.1 Thesis Overview

This thesis mainly focuses on the laser light scattered by Brownian particles as the object and studies its coherence properties through different photon correlation methods.

Chapter 2 introduces the theory and experimental methods of dynamic light scattering, a classical scattered light measurement method. Through theoretical analysis, we found that there are several parameters in the experiment that affect the coherence properties of scattered light and change the coherence time. Because it will generate both multiple scattering and single scattering when light propagates into the suspension, we discuss several measures to reduce the occurrence of multiple scattering in experiments.

Chapter 3 introduces the theory and experimental methods of the second-order coherence function $g^{(2)}$ which is the classic method for measuring the coherence properties of any light source. For the measurement of scattered light, the theory in Chapter 2 shows that the coherence properties depend on several parameters. In the experiment, we changed these parameters and measured the second-order coherence function to confirm the correctness of the theory and learn to control the coherence time of scattered light by analyzing the result.

Chapter 4 introduces the interferometric photon correlation method to measure the second-order coherence function which can be called $g^{(2X)}$. Compared with

the classic second-order coherence function, this measurement method can measure the coherence time of the phase jump of the laser and the decoherence terms of $g^{(2X)}$ function can be used to distinguish chaotic light and pseudothermal light. In addition, after the time delay between two beams, it can be used to separate amplitude fluctuations and phase fluctuations in $g^{(2X)}$ plot. In the experiment, we measured the $g^{(2X)}$ image of the laser and scattered light, analyzed the coherence characteristics, and summarized the shortcomings in the current experiment and the next step of research.

Chapter 2

Dynamic Light Scattering Techniques

Dynamic light scattering (DLS), also known as photon correlation spectroscopy, is a physical approach widely used to measure the size distribution characteristics of tiny particulates in a suspension or polymers dispersed in a solution. This technique also can be used to analyze the coherence properties of scattered light collected in a correlation system. This chapter introduces what coherent information can be obtained from the single scattering of dynamic light scattering and how it is related to properties of sample. Furthermore, there are specific methods that can reduce the impact of multiple scattering on DLS measurements in experiments.

2.1 Single Scattering

The most widely accepted explanation of DLS measurement is the single scattering hypothesis, in which all photons encounter and scatter at most one scattering particle with the same clearly recognized scattering vector and are directly detected by the detector. In this case, the intensity of the scattered light - the decreasing parameter of the intensity $G(\tau)$ autocorrelation function is usually directly related to the Brownian motion of the scattered particle. The following formula 2.1 illustrates the autocorrelation function of scattered light under an ideal experimental condition involving identical diffusion particles with a diffusion coefficient of D, based on the Siegert relation [10].

$$G(\tau) = 1 + \beta \left\{ exp(-Dq^2\tau) \right\}^2 \tag{2.1}$$

The exponential decay, in relation to the delay time as τ, represents coherence loss due to the Brownian motion, influenced by a diffusion coefficient D, and a wave

vector q. The coefficient β, as we mentioned before1.2, defined as the signal-to-noise ratio, illustrates the overall efficiency of optical detection, also commonly referred to as the coherent factor.

In a more detailed version of the equation, the exponential decay, Highlighted by brackets, could be replaced by integrating variations of and from diverse particles or scattering vectors. The equation 2.2 to determine the scattering vector is referred to below

$$q = \frac{4\pi n}{\lambda} \sin \frac{\theta}{2} \tag{2.2}$$

where n represents the refractive index of the solvent, λ is the wavelength of the laser, and θ is the scattering angle related to the direction of the irradiated light and the detector. Describe the second-order coherence function and Siegert function formed of the scattered light by Brownian particles, resulting in pseudothermal light.

The translational diffusion coefficient D is affected by the decay rate of the exponential decay function of each scattering of light by a particle, which is derived from the particle's viscous resistance to fission heat energy. This is also known as the Stokes-Einstein equation [11].

$$D = \frac{k_B T}{6\pi\eta R_H} \tag{2.3}$$

While η is the viscosity of the dispersant, T is the absolute temperature, K_B is the Boltzmann constant, and R_H is the radius of the particle. Therefore, it can be inferred from the theoretical model of single scattering that the autocorrelation function is related to a variety of features in the sample, such as temperature, the viscosity of the solvent, particle size, and detection direction. In experiments, changes in these influencing parameters can be observed to verify the correctness of the autocorrelation function and to determine the magnitude of a specific parameter to measure the other properties of the sample.

2.2 Multiple Scattering

Precise measurement becomes exceptionally challenging for systems where multiple scattering contributions are significant. In the DLS technique, we measure

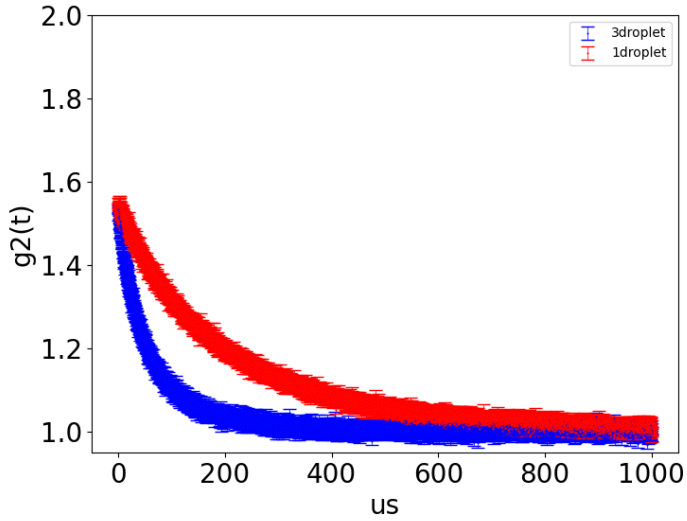

Figure 2.1: The coherence function of light scattered by aqueous 0.2um microsphere at different concentrations. In the same cuvette, for 3 drops of solution sample (blue) the coherence time is 61.5us with an amplitude of 0.48, and the coherence time is 196us with an amplitude of 0.51 for one drop (red).

how scattered light particles relate to each other on a short time scale. When light scatters multiple times, this increases the randomness of the signals we receive, which lessens their correlation. As a result, it makes the particles look as though they are moving quicker than their actual rate. In order to more accurately measure the coherence properties of light from single scattering, it is necessary to reduce multiple scattering in the sample during the experiment. There are some measurements to decrease the proportion of multiple scattering in the experiment.

Reducing concentrations of the sample. In DLS measurements, effects of high concentration on multiple scattering include: (1) When the sample's concentration increases, we see a drop in the intercept (or amplitude) that we measure as part of the correlation function; (2) As concentration goes up, we see that the perceived size of our sample goes down, which in turn reduces the coherence time of scattered light; (3) At higher concentrations, the distribution of multiple scattering increases. The provided figure2.1 demonstrates the effects of high concentration on the coherence function measurement of the solution by comparing the coherence functions of the solution under different concentrations.

By making the distance between the center of scattering and the detector

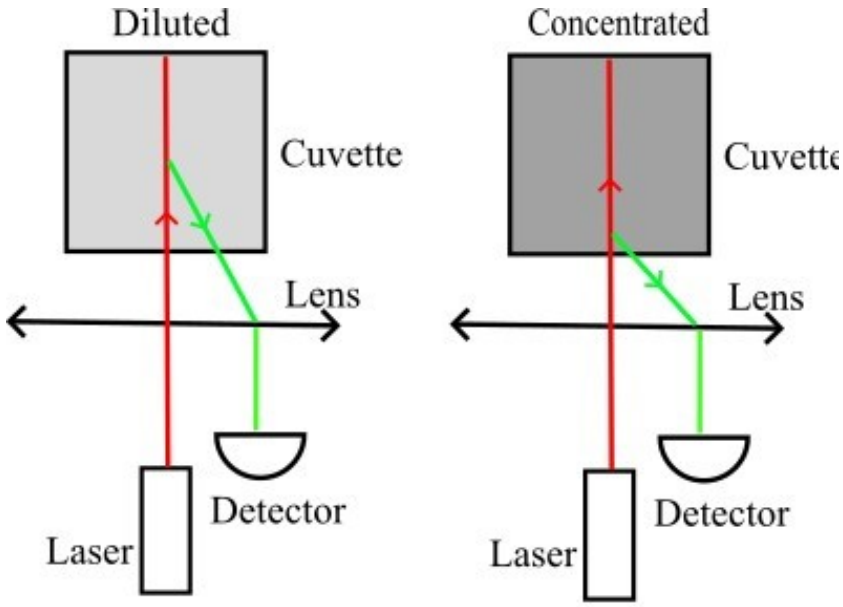

Figure 2.2: Pathway of light of different concentrations in suspensions.

shorter, one can effectively lessen the undesirable effects of multiple scattering. It is particularly beneficial to maximize single scattering when dealing with small particles or samples that have a lower concentration. The "flare" occurring as the laser light spreads through the surface of the cuvette and enters the dispersant might have the potential to overpower the scattering signal. One can counteract this phenomenon by setting the point of measurement from the position close to the surface of the cuvette towards its center. Larger particles or high concentration samples have the ability to scatter an increased amount of light. Under such circumstances, conducting measurements nearer to the surface of the cuvette can reduce the influence of multiple scatterings by effectively limiting the distance the scattered light must travel.

The setup for dynamic light scattering often involves a vertically polarized laser beam illuminating the sample. The scattered light is captured and the resulting intensity fluctuations are analyzed. The introduction of a polarizer between the sample and the detector influences the observed light scattering intensity, which depends on its orientation with respect to the scattering plane. According to Ragy Ragheb's correlation study on milk[12], the presence of a parallel polarizer before the detector amplifies the single scattering's relative impact. Conversely, a perpendicular

polarizer will diminish it. As a result, the incidence of multiple scattering can be suppressed in experiments by positioning a pair of parallel polarizers.

In conclusion, the approaches to alleviate the effects of multiple scattering on coherent function measurements can be summarized in these three types: diluting the solution concentration, adjusting the direction of the light pathway between the laser and the detector, and introducing a pair of parallel polarizers before the detector in the experiment.

2.3 Summary

This chapter introduces single scattering and multiple scattering in dynamic light scattering technology. The coherence function of single scattering is related to the temperature of the sample, the viscosity of the solvent, particle size, and scattering angle. In the experiment, changes to these parameters can achieve changes in coherence time. Multiple scattering is hoped to be avoided in the measurement of the coherence function of scattering light. In the experiment, we can reduce the occurrence of multiple scattering by diluting the solution, adjusting the pathway of the light, and adding a pair of parallel polarizers.

Chapter 3

Second Order Coherence Time Measurement

The $g^{(2)}$ function, essential in the exploration of light's particle properties, has become a key player in this rapidly advancing field. Based on the concepts of photon bunching and antibunching phenomena, $g^{(2)}$ measurements not only just demonstrate our understanding of the quantum properties of light but have found wide-ranging applications, significantly influencing the fields of telecommunications, diagnostic medicine, environmental sensing, etc.

This chapter primarily introduces the theory of second-order temporal coherence function, as well as the measurement of the $g^{(2)}$ function of laser light and laser light scattering by microspheres in suspension fluid, based on the theory of the Hanbury Brown and Twiss (HBT) experiment. Also, according to dynamic light scattering (DLS) theory, by changing the parameters of the sample in the experiment, we compare changes to the second-order coherence function and consider how to reduce the coherence time to provide feasibility for the measurement of interferometric photon correlation experiments in practice.

3.1 Theory

One could say that the first-order correlation function often noted as the temporal field correlation function $g^{(1)}(\tau)$, is one of the key methods used to detail coherence properties. This function essentially provides a measurement or description of how related or similar the field is at different points in time, which is defined as

$$g^{(1)}(r_1, t_1; r_2, t_2) = \frac{\langle E^*(r_1, t_1) E(r_2, t_2) \rangle}{[\langle |E^*(r_1, t_1)|^2 \rangle \langle |E(r_2, t_2)|^2 \rangle]^{\frac{1}{2}}} \tag{3.1}$$

Where $\langle ... \rangle$ denotes a statistical ensemble average. In the case of non-stationary states like pulses, with a group composed of multiple pulses. When working with stationary states, which exhibit unchanging statistical properties over time, the group average can be substituted with a time-based average. Further, if limiting the waves that are parallel to one another, then correlation distance will equate to distance along the z-axis $r = z$. In this case, the coherence function for stationary states will not depend on t_1, but on the time difference $\tau = t_1 - t_2$. Hence, $g^{(1)}(\tau)$ can be written to a simplified form

$$g^{(1)}(\tau) = \frac{\langle E^*(t)E(t+\tau)\rangle}{\langle |E(t)|^2 \rangle} \tag{3.2}$$

With $\langle ... \rangle$ relating to the averaging over the time t and field $E(t)$. Generally, the function $g^{(1)}(\tau)$ is set at 1 when $\tau = 0$ and it diminishes to 0 when τ is large, indicating a total uncorrelation between the electric fields. The average decline time is representative of the electric field's coherence time, denoted as τ_c.

Since Glauber's seminal work[13], it is been widely recognized that to entirely characterize a light source's coherence properties, it is necessary to measure the correlation functions $g^{(n)}(\tau)$ at every order n. The measurement of $g^{(2)}(\tau)$ can reveal various characteristics of light, including its intensity correlations, statistical properties of photons, fluctuations of the light source, and potential non-classical behaviors. In general, $g^{(2)}(\tau)$ is primarily used to examine the statistical properties and coherence of light. According to the $g^{(1)}(\tau)$ coherence function in the stationary field, if the electric fields are considered classical, a plane parallel wave in a stationary state will have

$$g^{(2)}(\tau) = \frac{\langle I(t)I(t+\tau)\rangle}{\langle I(t)\rangle^2} \tag{3.3}$$

Typically, the brackets suggest a time-based average, but they can be swapped with a group average for light fields that are not changing. If one were to record the variations in intensity over a period, we could explain $g^{(2)}(\tau)$ as the standardized autocorrelation function of brightness. It is possible to prove that for traditional fields, $g^{(2)}(\tau)$ is always greater than or equal to 1 and that $g^{(2)}(0)$ is equal to or greater than $g^{(2)}(\tau)$.

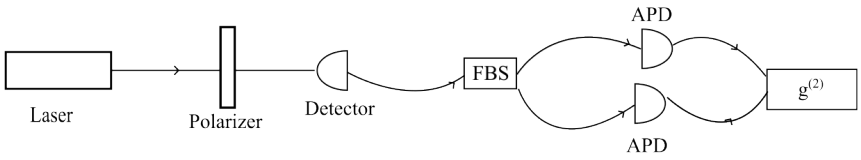

Figure 3.1: setup for measuring the second-order coherence function of laser light

3.2 HBT experiment

The Hanbury Brown-Twiss(HBT) experiment is a common method for measuring second-order coherence functions in the laboratory. The primary subject of the HBT experiment, also referred to as an intensity interferometry technique, centers on the exploration of photon bunching or coincident detection of photons. This process involves using two detectors to simultaneously record photon statistics at two positions, thereby determining photon correlations within the light beam. When photons possess a common source, the probability of coincident detection is higher than that of random events, thereby aiding the observation of robust photon bunching.

3.2.1 Laser

Before proceeding with the measurement of the second-order coherence function of pseudothermal light, we first used the HBT experiment to measure the second-order coherence function $g^{(2)}(\tau)$ of the lasers to verify the stability of the lasers. If the second-order coherence function of the laser remains steady and the $g^{(2)}(\tau)$ measurements are around 1, this indicates that the laser can produce a stable coherent light source.

The figure 3.1 shows a simple setup for measuring the second-order coherence function of laser in the experiment. We used a 633nm He-Ne laser as the light source. It was polarized by a linear polarizer with an extinction ratio of 1:1000 and then collected into a single-mode optical fiber through a focus lens. After passing through a 50:50 fiber beamsplitter, the light was collected by two silica avalanche photo detectors (APDs), and counting the coincidence of photons received by the two APDs through the timestamp counter. Finally, the second-order coherence function

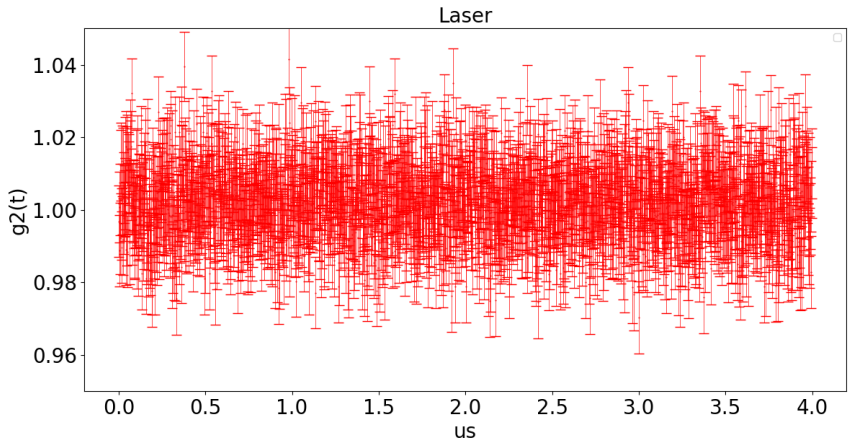

Figure 3.2: Second-order coherence function of the stable coherent laser field.

can be calculated from the coincidence in different channels of the two APDs.

The figure 3.2 shows the second-order coherence function $g^{(2)}$ plot of the He-Ne laser on a time scale of 4 microseconds. It can be seen that during this period of time scale, the $g^{(2)}$ value shows a flat shape and fluctuates near 1, indicating that the laser is sufficient as a stable coherent light source and can be used as a basic light source in dynamic light scattering experiments.

3.2.2 Microsphere suspension

As a more affordable scattering fluid with similar properties and readily available Brownian particles in everyday life, we initially employed this sample as a standard microsphere suspension in the experiment to assess the second-order coherence function in DLS technology. Milk solution contains microscopic fat globules, which undergo comparable Brownian motion also studied with photon correlation spectroscopy [14]. Since milk presents a much more economical resource compared to other commonly used materials in DLS experiments, it was chosen in the early stages of experiments to observe the scattering patterns of laser light scattered by it. The figure 3.3 shows the setup used in the experiment to measure Brownian particles such as milk. A 633nm He-Ne laser was used as the light source. Two parallel polarizers with an extinction ratio of 1:1000 and a focus lens with a focal length of 10cm were used to focus the light in the middle of the cuvette to adjust the impact of multiple scattering on the results. In the experiment, the reflection direction

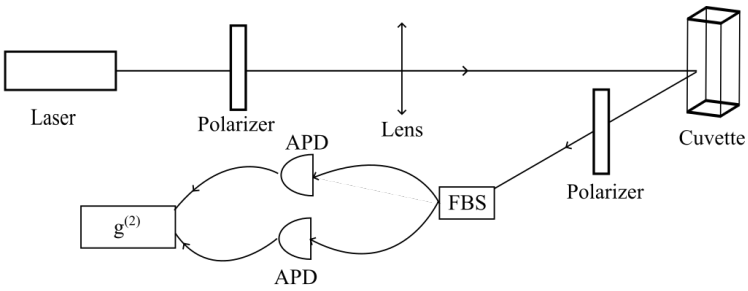

Figure 3.3: Setup for measuring second-order coherence function $g^{(2)}$ of milk

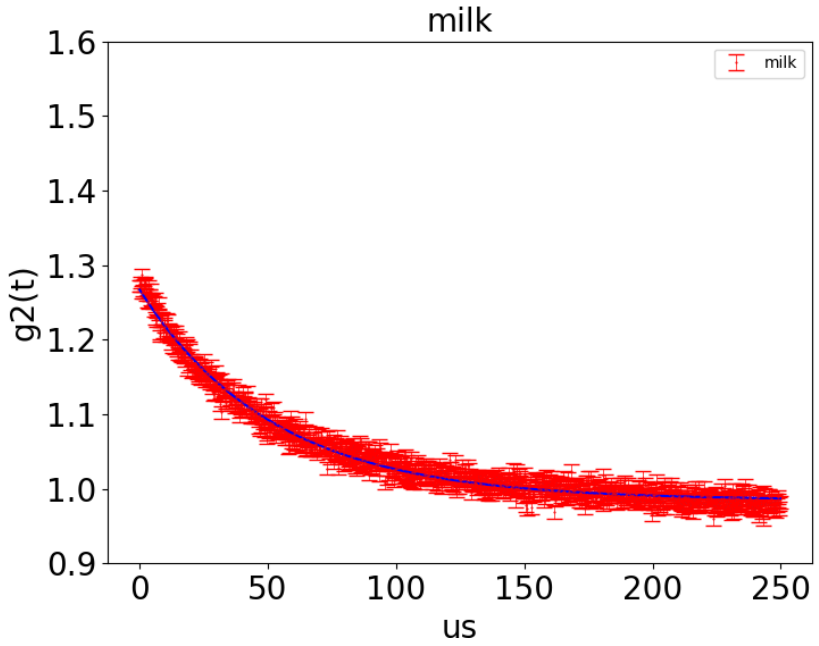

Figure 3.4: Second-order coherence function of Milk

commonly used in dynamic light scattering was selected to collect the scattering light, and the scattering angle was approximately 150 degrees. And a 50:50 fiber beamsplitter and two APDs were also used to form the HBT experimental method to measure the second-order coherence function $g^{(2)}$ of scattering light. The figure 3.4 below is the result we obtained using milk as a test for measuring $g^{(2)}$ of Brownian particles.

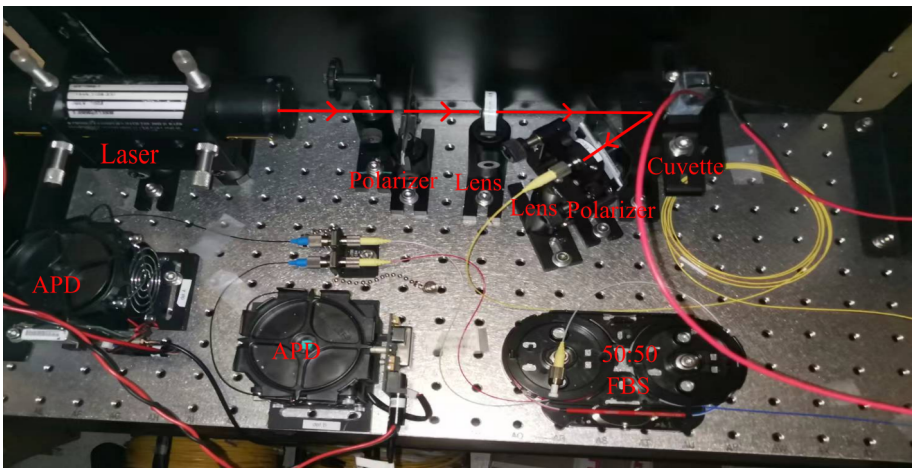

Figure 3.5: Experimental setup for measuring $g^{(2)}$ function of microsphere

3.3 Parameter of second-order coherence of microsphere

The coherence time is a crucial characteristic when studying the second-order coherence function. As mentioned in Chapter 3, the coherence time of scattered light is related to parameters of the sample such as viscosity of solution, size of the particle, temperature, scattering angle, and laser wavelength. In experiments, if the coherence time of scattered light by a suspended liquid sample is measured, it can be used to measure the parameters of the sample conversely. This application is widely used in fields such as chemistry, biology, medical. In addition, as we will introduce in the next section, the time delay in interferometer photon-correlation measurement depends on the coherence time of the scattered light. Therefore, a clear understanding of the influence of sample parameter changes on the second-order coherence function of scattered light is an important basis for the next step of research. In this section, we will mainly discuss how changes in different parameters affect the second-order coherence function of the scattering light.

As the theoretical basis for the experiment, it is necessary to verify the correctness of Equation 2.1 first. The following image shows an experimental setup, which uses the same dynamic light scattering measurement method as Figure 3.3. We measured the second-order coherence function of 0.22 μm diameter polystyrene microspheres in distilled water as a solvent, with a scattering angle close to 150 degrees. As shown in figure 3.6, according to the predictions of the equation, in an environment with

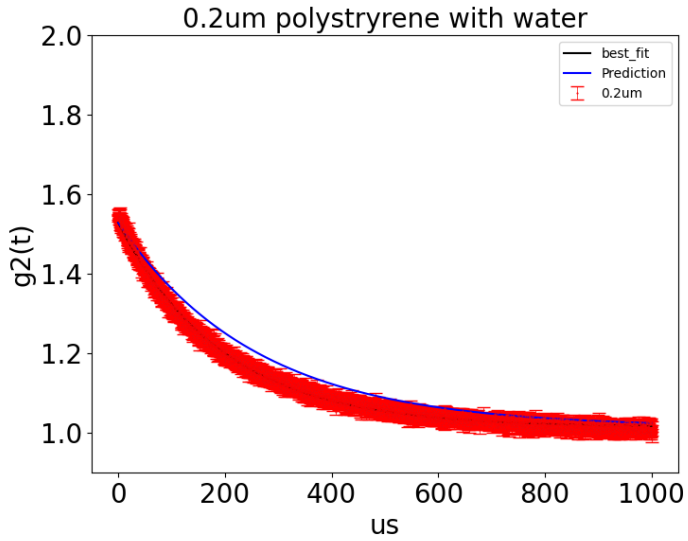

Figure 3.6: Measuring the second-order coherence function of a 0.2-micron microsphere in distilled water, reappears the result from the literature to prove the experimental correction.

a laboratory temperature of approximately 28 Celsius, the coherence time of the scattered light should be about 227 μs. In the experiment, after fitting the obtained data using a Lorentzian distribution, the coherence time of scattering light is about 198 μs. Comparing the measured coherence time with that obtained from similar measurements in the literature[15], it can be seen that the coherence time lies in the same range of values, confirming the appropriateness of our experimental process and the validity of the theoretical equation for DLS. The observed deviation in the coherence time may be due to the impossibility of completely eliminating multiple scattering effects in the experiment, which would result in a lower coherence time being measured.

3.3.1 Diameter of microsphere

In the experiment, two types of microsphere materials were chosen: silica colloid with a diameter of 20 nm, and polystyrene with a diameter of 0.22 μm. The coherence time of the scattered light from a 633-nanometer He-Ne laser was measured under identical conditions: distilled water as the solvent, at room temperature, and at a scattering angle close to 150 degrees. After fitting the data, the coherence times obtained were 25 μs and 198 μs, respectively. Thus, this illustrates that reducing

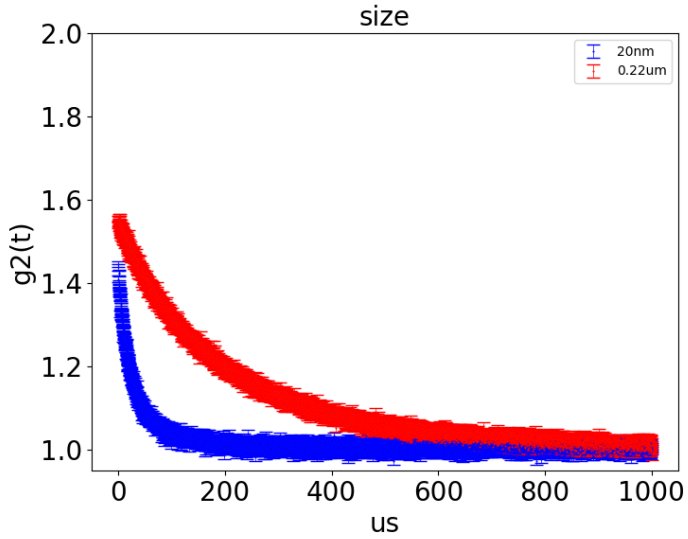

Figure 3.7: Changing the diameter parameter of microsphere suspension to observe how this parameter effected on the second-order coherence function.

the particle diameter by one order of magnitude also reduces the coherence time by approximately one order of magnitude, which is also evidence for the formula.

3.3.2 Viscosity of solvent

According to literature[16], the viscosity of the coffee solution is greater than that of distilled water. In the experiment, we increased the viscosity of the solvent by adding a few drops of black coffee solution to distilled water. From the measurement results, we can see that when the viscosity of the solution increases, the coherence time will also increase. When adding coffee, we used a power meter to reduce the laser's transmission to 10 percent of the original. The second-order coherence function measured at a scattering angle of 150 degrees indicates that the decrease in laser transmission in the solution will result in a decrease in the light intensity measurement of scattered light in the reflection direction, but it will not make it impossible to measure the $g^{(2)}$ image. Furthermore, by comparing with the results of silica colloid measurements, since the silica microspheres in the solution are transparent compared to the white polystyrene microspheres, the collected light intensity also decrease. Therefore, the reduction of the intensity of scattering light may related to the decreasing peak of $g^{(2)}$ at zero time difference in the experiment.

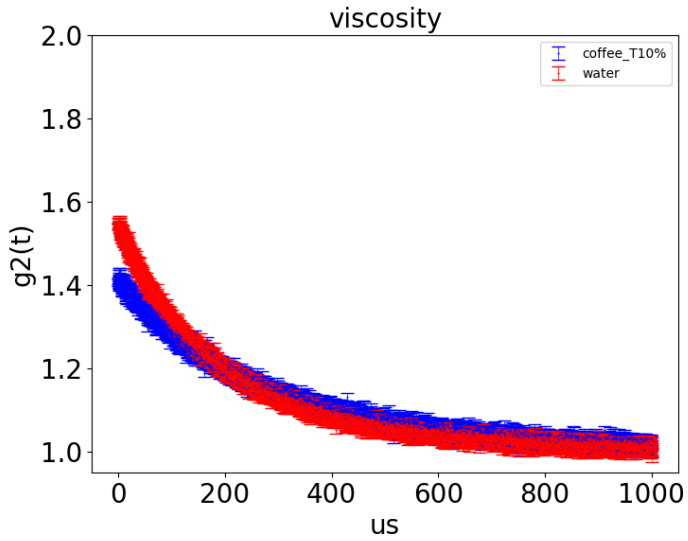

Figure 3.8: Changing the Viscosity of solvent to observe how this parameter effected on the second-order coherence function.

3.3.3 Temperature

In the experiment, an oven controller was used to heat the solution in a cuvette from the bottom using a heating resistor, and the temperature within the solution was measured with a thermistor, thus effectively controlling the temperature of the solution in the cuvette. As the temperature rises during heating, not only is the thermal motion of the microsphere particles in the solution increased, but the viscosity of the solution is also reduced[17]. Changes in both parameters will reduce the coherence time. The experiment compared the second-order coherence function of a 633 nm He-Ne laser through a 20 nm silica colloid aqueous solution at room temperature of 27 Celsius and 70 Celsius. At 70 Celsius, according to the table in the literature, the viscosity is 0.4035 $mpa.s$. According to the calculation, the coherence time obtained at 70 Celsius was 10.3 microseconds. The result of the experiment obtained by fitting the data was that the coherence time of the scattered light was 11.5 microseconds. This confirms that the coherence time decreases when the temperature of sample is increased.

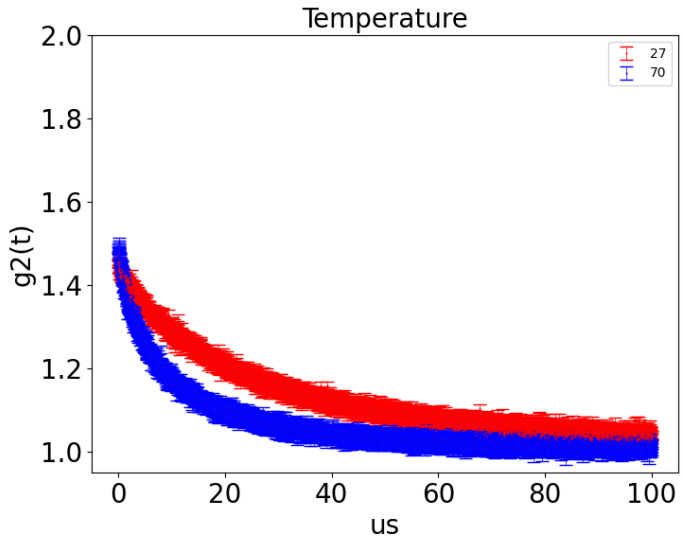

Figure 3.9: Changing the temperature will simultaneously affect the viscosity of the solvent and the dynamic motion of Brownian particles, thereby altering the second-order coherence time.

Temperture[$°C$]	27	28	29	30	40	50	60	70	80
Dyn.Viscosity[mPa.s]	0.8509	0.8324	0.8145	0.7972	0.6527	0.5465	0.466	0.4035	0.354
Kin.Viscosity[mm^2/s]	0.8539	0.8355	0.8178	0.8007	0.6579	0.5531	0.474	0.4127	0.3643
Density[g/cm^3]	0.9965	0.9962	0.9959	0.9956	0.9922	0.988	0.9832	0.9778	0.9718

Table 3.1: The viscosity and density of water change with temperature. Data extracted from[18]

3.3.4 Scattering angle

In the experiment, the scattering angle of the scattered light was varied by changing the direction of the collected light entering the optical single-mode fibre. Measurements were made at room temperature of the second-order coherence function of scattered light at scattering angles of approximately 150 degrees figure 3.3.4 and 18 degrees figure 3.3.4 in the reflection direction, respectively. It resulted in coherence functions that differ by about 40 times. Since the scattering angle is a relevant parameter of the scattering vector in the equation, it has a square relationship with the coherence time. According to the values of $\sin 75°$ and $\sin 9°$, the changes in coherence time can correspond to the two scattering angles. This confirmed that the

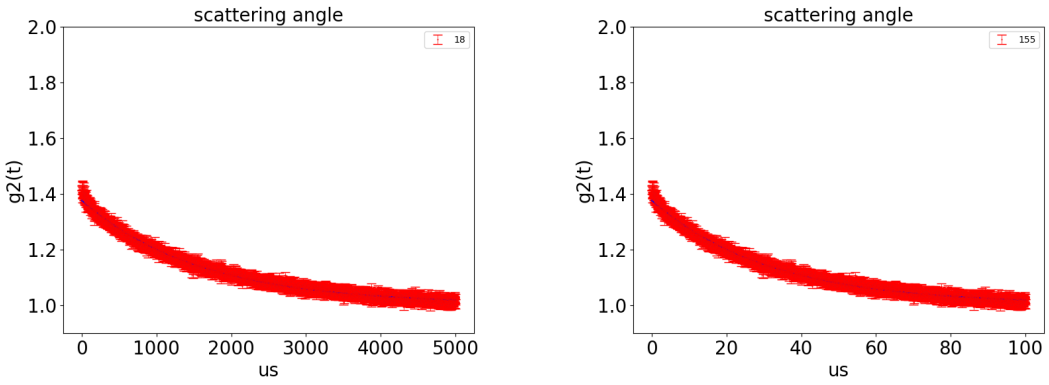

effect of the scattering angle parameter on coherence time conforms to the inference of the dynamic light scattering theory.

3.4 Summary

This chapter mainly introduces the basic theory of the second-order coherence function $g^{(2)}$ and the basic experimental method (HBT experiment) for measuring the second-order coherence function of the light source. In the experiment, because the laser is a stable coherent light source, the second-order coherence function of the laser is always flat to the value of 1. Scattering light by Brownian particle will cause photon bunching phenomenon at 0 time delay which means $g^{(2)}(0) > 1$. The second-order coherence function of scattered light satisfies Gaussian distribution and the coherence time of scattered light can be obtained from $g^{(2)}$. According to DLS theory in Chapter 3, the coherence time of scattered light depends on several experimental parameters. In the experiment, we analyzed the variation of coherence time by changing relevant parameters and laid the foundation for the content of cross correlation measurement on coherence time.

Chapter 4

Cross Second-order Coherence Time

As a definition of the second-order coherence function, the peak value of the second-order coherence function $g^{(2)}(0)$ mainly quantifies the variance within the intensity modulation and does not extend to distinguish whether the electric field of the measured source is a statistical set of random phase jumps or a coherent state with amplitude modulation. This property has been observed in coherent laser fields. When there are phase or amplitude fluctuations (as observed in pseudothermal light produced by laser scattering through rotating ground glass or microsphere suspensions), $g^{(2)}(0)$ is usually larger than 1. Thus, $g^{(2)}(\tau)$greater than 1 is not a decisive feature of the chaotic spontaneous independent emission of the existence of thermal light.

To solve this problem, Lebreton [19] demonstrates an interference cross-correlation technique that clearly distinguishes the above light sources. Originally developed to study spectral diffusion in molecules, this method requires measuring the cross-intensity coherence between two beams of a non-equilibrium Michelson interferometer while operating in an experimental photon counting system and averaging across numerous fringes and time periods. The application of this technique accommodates the theoretical exploration of interferometric photon correlation experiments and the assessment of the corresponding correlation functions among three kinds of electromagnetic field conditions: chaotic light such as thermal light, stable coherent light such as laser light, and amplitude-modulated coherent light such as pseudothermal light. The findings exhibit significant differences in the intensity correlation function between chaotic light and coherent light, suggesting that coherent light has distinct characteristics. This reveals that even with similar first and second-order correlation functions, chaotic and amplitude-modulated coherent lights can be differentiated

through their respective cross-intensity correlation functions.

Based on the interferometric cross-correlation experimental method, this chapter will introduce its basic theory. Then, through theoretical derivation, we will introduce the cross-correlation function $g^{(2X)}(\tau)$ image of the laser and the pseudothermal light after the laser is scattered by the microsphere suspension. And comparing the images we measured in the experiment to analyze the properties related to the phase and amplitude fluctuation of the scattered light.

4.1 Theory

The expression of the second-order intensity cross-correlation function obtained by the coherent calculation of two output segments of the Michelson interferometer can be expressed as follows:

$$g^{(2X)}(\tau, \sigma) = \langle E_A^*(t) E_B^*(t+\tau) E_B(t+\tau) E_A(t) \rangle_t \tag{4.1}$$

In this case, τ represents the time difference between pairs of photon detection events, and $\sigma = d/c$ reflects the "interference delay", the path difference is similar to $\sigma c/n$ between the two arms of the interferometer (where c is the speed of light in vacuum and n is the refractive index of the optical fiber). E_i^*/E_i is a way of showing the components of the electric field operator that involve both positive and negative frequencies at the output port, which can be either A or B. Here, $\langle ... \rangle_t$ represents The quantum mechanical and statistical average, while the change of the time mean over time t is normalized by the divisor to $g^{(2X)}(\tau)$. Output fields can be represented using input field operators as

$$\begin{aligned} E_A^*(t) &= \frac{a^\dagger(t+\sigma) - a^\dagger(t)}{\sqrt{2}} \\ E_B^*(t) &= \frac{a^\dagger(t+\sigma) + a^\dagger(t)}{\sqrt{2}} \end{aligned} \tag{4.2}$$

In the context of quantum mechanics, the creation operator denoted as $a^\dagger(t)$, plays a crucial role in managing the input mode. It is important to note that identical equations may be written for E_A/E_B and annihilation operators. Equation

4.1 can be developed further into sixteen distinct parts. In this equation, ten of the terms typically average to a null value when the difference within the interferometer arm (noted as $\sigma c/n$) is dithered by a few wavelengths. The six remaining terms are as follows

$$\begin{aligned} g^{(2X)}(\tau,\sigma) =& \frac{1}{4}\langle a^\dagger(\sigma)a^\dagger(\sigma+\tau)a(\sigma+\tau)a(\sigma) \\ &+ a^\dagger(0)a^\dagger(\tau)a(\tau)a(0) \\ &+ a^\dagger(0)a^\dagger(\sigma+\tau)a(\sigma+\tau)a(0) \\ &+ a^\dagger(\sigma)a^\dagger(\tau)a(\tau)a(\sigma) \\ &- a^\dagger(\sigma)a^\dagger(\tau)a(\sigma+\tau)a(0) \\ &- a^\dagger(0)a^\dagger(\sigma+\tau)a(\tau)a(\sigma)\rangle \end{aligned} \tag{4.3}$$

The first two components of this equation pertain to the function $g^{(2)}(\tau)$, which is commonly referred to as the standard second-order autocorrelation function of the input field. This double photon propagation is similar to particle-like movement along identical arms of the interferometer. The third and fourth terms, on the other hand, respectively correspond to the functions $g^{(2)}(\tau+\sigma)$ and $g^{(2)}(\tau-\sigma)$. These explain the propagation of two photons acting as particles along diverse arms of the interferometer. These four factors only account for changes in light intensity within the field. The last two elements, represented by a negative sign, summarize the changes in the field as it undergoes interference when passing through both arms of the measuring tool known as the interferometer at the same time. Compared with their preceding counterparts, these sections are also sensitive to potential modulation in both amplitude and phase. These six components pertain to the conditional probability of observing a second photon at time $t=\tau$ given that there is constructive interference of the two pathways with a difference d, leading to the first photon detection at $t=0$. As a result, it can be possible to reconstruct Equation (7) as

$$\begin{aligned} g^{(2X)}(\tau,\sigma) =& \frac{1}{4}\langle 2g^{(2)}(\tau) + g^{(2)}(\sigma+\tau) \\ &+ g^{(2)}(\sigma-\tau) - 2Re[g^{(2)}(d/c,\tau,d/c+\tau,0)]\rangle \end{aligned} \tag{4.4}$$

$g^{(2)}(t_4, t_3, t_2, t_1) = \langle a^\dagger(t_4)a^\dagger(t_3)a(t_2)a(t_1)\rangle$ represent the four-time second-order coherence function of the input field as the "interference terms". According to the equation 4.4 above, in the following section we introduce the cross-correlation function $g^{(2X)}(\tau)$ of laser light and the pseudothermal light generated after the laser light is scattered by the microsphere suspension, as well as the measurement results obtained in the experiment.

4.2 Laser

When a laser operates above its threshold, the light it produces can be described as a coherent quantum state. This state is a superposition of all states of the laser mode, with an expected value greater than zero in the electric field operator and oscillations [20]. At this point, the laser's electric field refers to a typically stable oscillating wave.

In this case, the laser field can be represented by the Schawlow-Townes process exemplifying phase diffusion. This process can also be seen as brief, sudden, and random jumps in the phase of the fluctuating coherent field. Within these bounds, the area showcases a pure quantum coherent state and the electric field operator exhibits non-zero oscillations. This contradicts chaotic fields, where in the electric fields consistently average to zero, as identified while determined the electric field equations for spontaneous and independent emitters [21]. The electric field generated by a conventional laser can be expressed as follows.

$$E^*(t) = E_1^* e^{i\omega t + i\phi(t)} \tag{4.5}$$

The term $E_1^* = E_0^*\sqrt{\langle a^\dagger a\rangle}$ represents the coherent amplitude of the electric field, where E_0^* is its average value and $\langle a^\dagger a\rangle$ denotes the expectation value of the number operator which gives the average number of photons in the state. The phase ϕ of the field experiences random jumps with a correlation time that corresponds to the Schawlow-Townes phase diffusion time. This time scale τ characterizes the rate at which the phase of the oscillation randomly fluctuates.

Because we are considering a single electromagnetic mode in a coherent state rather than an ensemble of waves, the statistical average$\langle ...\rangle$ is actually an average

of the random phase jumps over time. The first correlation function of this field gives us insights into these phase fluctuations and their impact on the coherence of the field as

$$g^{(1)}(\tau) = e^{i\omega\tau}\langle e^{i\phi(\tau)-i\phi(0)}\rangle = e^{i\omega\tau}e^{-|\tau|/\tau_\phi} \tag{4.6}$$

The second-order coherence function of conventional laser light is

$$g^{(2)}_{coh}(\tau) = 1 \tag{4.7}$$

Showing the stable coherence condition of the laser light and the absence of photon bunching. After designing the time delay of one of the laser beams in interferometric measurement, The interference terms in $g^{(2X)}$equation4.4 could be calculated as

$$\begin{aligned} g^{(2)}(\tau,\sigma,\tau,0) &= \langle e^{i\phi(\sigma)+i\phi(\tau)-i\phi(\sigma+\tau)-i\phi(0)}\rangle \\ &= e^{-2m/\tau_\phi} \end{aligned} \tag{4.8}$$

Where $\sigma = d/c$ is the time delay between the two beams. $m = min(|\sigma|, |\tau|)$ takes the smaller of the two values. According to equation 4.4, the interferometric second-order intensity cross-correlation function $g^{(2X)}$ for a stable coherent laser field with phase fluctuation can be written as

$$g^{(2X)}_{coh}(\tau) = 1 - \frac{1}{2}e^{-2m/\tau_\phi} \tag{4.9}$$

It composed by a flat baseline at $g^{(2X)}(\infty,\sigma) = 1 - \frac{1}{2}e^{-2d/(c\tau_\phi)}$, where there is a decrease to a $g^{(2X)}$ value of 0.5 at $\tau = 0$. This drop is a distinctive feature of coherent states and becomes especially significant when the interferometer is heavily unbalanced ($d >> c\tau_\phi$). In such situations, the baseline reaches its peak value of $g^{(2X)}(\infty,\sigma) = 1$. The full width, measured at $1 - 1/(2e) = 0.816$, directly indicates the correlation time τ_ϕ of a chance phase shift. The value at $\tau = 0$ (which is markedly less than 1), signifies that if the first photon is spotted in a specific

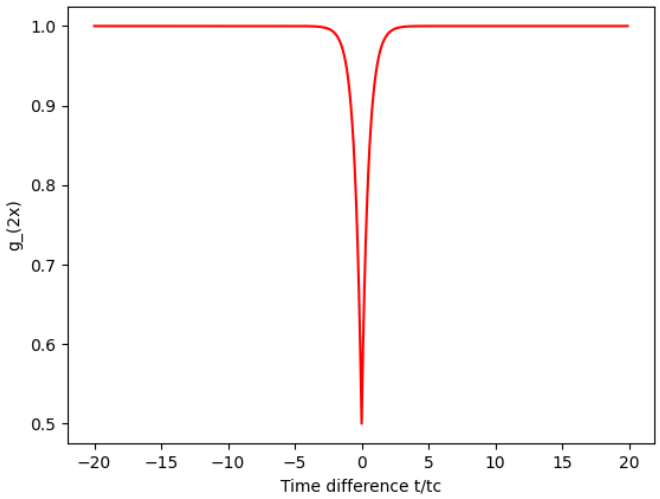

Figure 4.1: Second-order intensity cross-correlation function $g_{coh}^{(2X)}(\tau, \sigma)$ simulation for a stable coherent wave.

output port, the subsequent photon that arrives at time $\tau << \tau_\phi$ will exit via the same port. This is due to the coherent state maintaining its phase memory over these brief intervals, leading to constructive interference at the identical output. Yet, if a lengthy duration $\tau >> \tau_\phi$ is considered, a second photon could potentially leave through either port, resulting in a value of $g^{(2X)}(\infty, \sigma) = 1$. According to the equation, we can get the image of the autocorrelated second-order coherence function of the theoretically stable coherent light source as shown in the figure 4.1.

The figure 4.2 shows the setup for measuring the interferometric photon correlation of light from a laser diode with a central wavelength of around 658nm in our experiment. In the experiment, the laser intensity was adjusted by the attenuator to achieve the best measurement value in the experiment. The laser light is split into two beams through a 70:30 fiber beam splitter and one of the beams is delayed through a 400m fiber, which means $2\mu s$time delay between two beams, to form an asymmetric MachZehnder interferometer. Then the two beams are interfered through a 50:50 fiber beamsplitter. A half-wave plate and a quarter-wave plate composed by a fiber polarization controller are used to adjust the polarization directions of the two light beams to the same so as to achieve the interference of two beams. Finally, two actively quenched silica single photon avalanche photo diodes (APD) were used to collect photonevents to observe interferometric photon

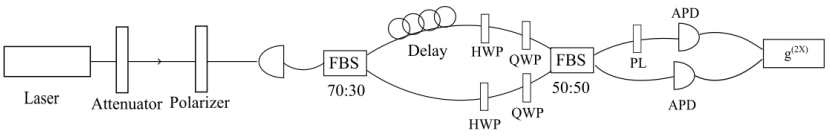

Figure 4.2: Theoretical setup for measuring second-order intensity cross-correlation function of light from laser diode

correlations in the second-order coherence function. The detected photoevents were time-stamped with a resolution of 2 ns for an integration time T .

The correlation function denoted as $g^{(2X)}$ is derived by numerically creating a histogram of all time differences $(t_2 - t_1)$ between detected pairs of events within a specified interval T. This approach enhances an effective normalization. The correlation obtained in the end is modeled using a two-sided exponential function. If the measurement time of one channel is fixed, the time difference can be written as $(t_2 - t_1) = \tau$. In this case, the cross second-order coherence function can be written as

$$g^{(2X)}(\tau) = 1 - Ae^{-\frac{\tau}{\tau_c}} \tag{4.10}$$

Here, τ_c denotes the characteristic time constant of the coherent light, with A indicating the amplitude of the dip. The value of $g^{(2X)}(0)$ is then determined from the fitting as $1 - A$. An illustration representing the actual setup used in the lab is also provided in figure 4.4.

In the experiment, the current of the laser diode was increased to 55mA with current above the lasing threshold to achieve a stable laser output state. In this case, a clear dip appears in the second-order coherence function plot by making a time delay between the two beams.

We used two NIM cables of 1m and 10m respectively to transmit the electric signals from two APDs to the timestamp card, hence advancing the second-order coherence function plot by approximately 40ns during the calculation to see the complete and obvious dip. Because the time delay from the longer fibre is much larger than the coherent time of laser light, the dip of cross second-order coherence function should be obviously observed. According to the interferometric photon

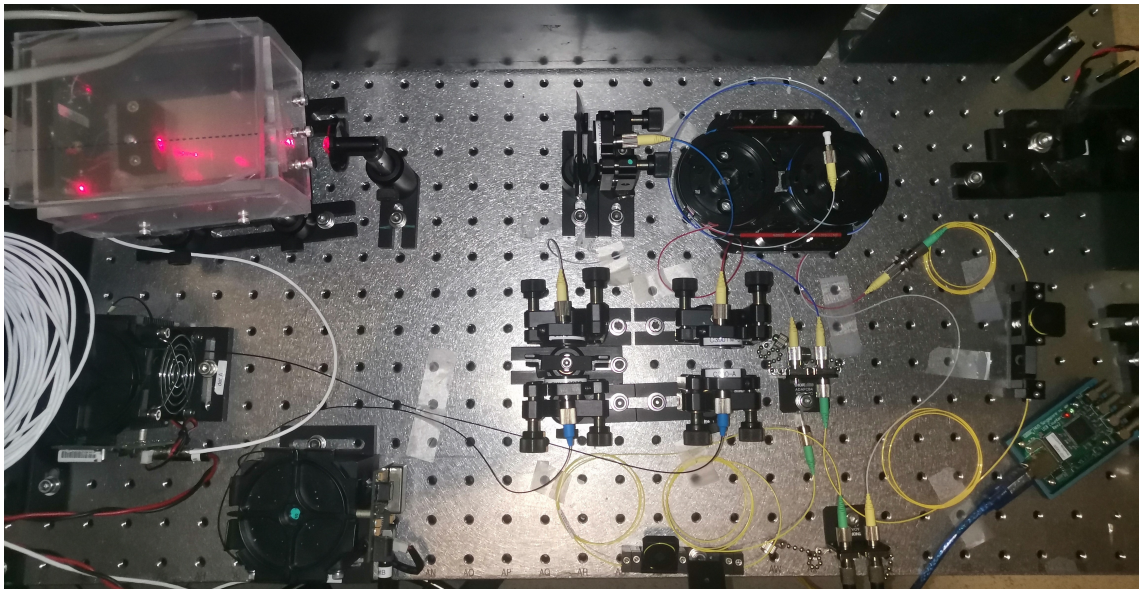

Figure 4.3: Actual setup for measuring second-order intensity cross-correlation function of light from laser diode in lab

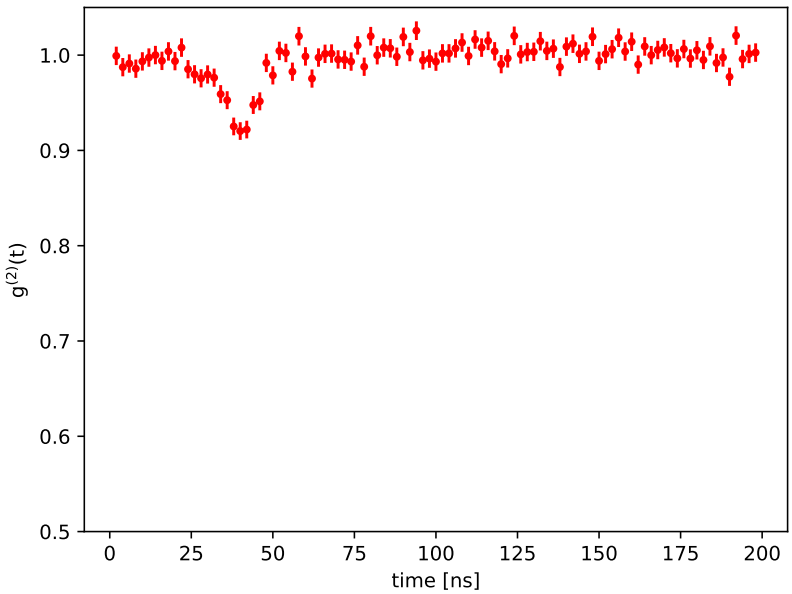

Figure 4.4: Interferometric photon correlations $g^{(2X)}$ for 55mA current laser diode.

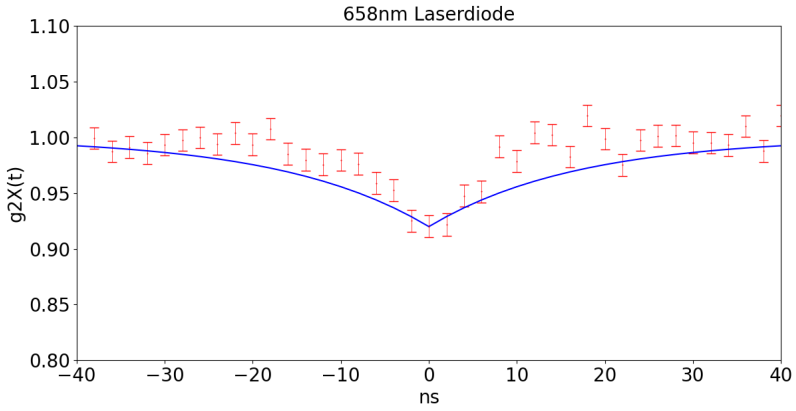

Figure 4.5: Zoom in the part of dip from figure 4.4. The amplitude of the dip $A \approx 0.0797$.

correlation formula 4.10, we zoom in on the part of the dip in figure 4.5 and fit it through the theoretical formula. Eventually, we get the characteristic time constant of the laser, which is nearly 33ns.

The reason why the lowest value of dip is 0.92 instead of the theoretical prediction of 0.5 may be caused by the following points: 1. The intensity of the two beams of light is unbalanced, resulting in a reduction in the amplitude of the dip. 2. Under this operating current, there is still a mixture of coherent and completely incoherent light, and thermal light from the laser diode, resulting in a reduction in amplitude. 3. According to the theoretical fitting, the coherence time of the laser is 33ns, and the resolution of the timestamp device is 2ns. When the coherence time is small and close to the resolution time, it will affect the measurement of its amplitude.

We also tried to use cross correlation measurement to measure the cross $g^{(2X)}$ image of the He-Ne laser. However, the He-Ne laser has an extremely narrow linewidth, allowing its coherence length to extend to the order of meters or even kilometers. In this case, it is difficult to find a fiber long enough to time delay the two beams. In the experiment, we tried to use a 400 meter optical fiber for a time delay of 2 us, which is still much smaller than the coherence time of the He-Ne laser. We measured on a very long time scale up to milliseconds and found that oscillation around the 1 value appeared at this time.

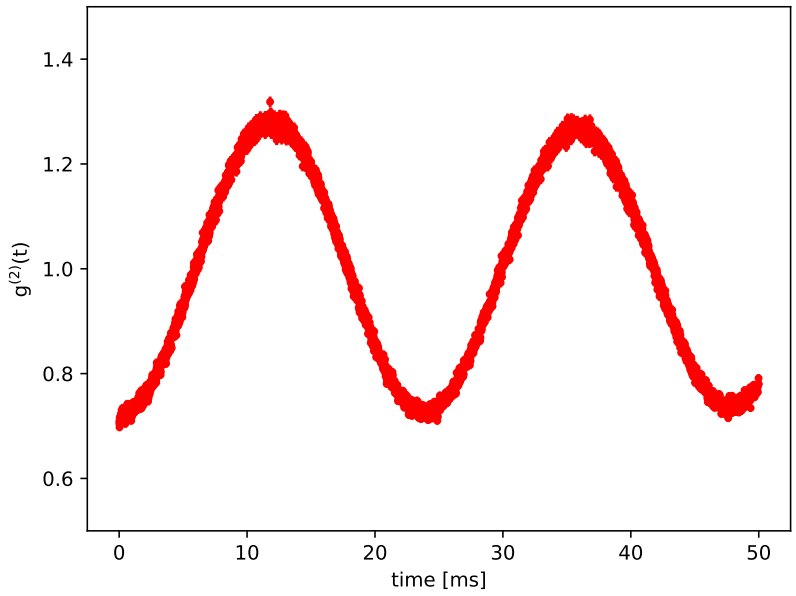

Figure 4.6: Interferometric photon correlations $g^{(2X)}$ for He-Ne laser.

4.3 Microsphere

Previous studies[22] have established the characteristics of the first-order or single scattered field by Brownian particles. If we take a plane wave $E_0 exp[i(k_0 r - \omega_0 t)]$ and illuminate the particulate solution with the light source, we can denote k_0 as the wave vector of this incoming light beam, and ω_0 as the wave's angular frequency. Under this light, every particle transforms into a radiating dipole moment. If we place a detector at a distance R from any point of reference within the illuminated area, the total electric field $E(t)$ detected is identified as the collective effect of fields radiated from each particle. For single scattering, it is given by

$$E(t) = E_0^{'} exp[i\phi_j(t) - i\omega_0 t] \tag{4.11}$$

Where $E_0^{'}$ is the amplitude of the electric field scattered by the Brownian particle. This amplitude is independent of the position of the particle but related to the following factors: the wave vector of the wave after scattering, the angle between the direction of propagation of the scattered wave and the direction of polarization, the difference between the dipole polarizability of the solvent and the particle and

the volume of the Brownian particle. The exact position of the single particle enters through the phase factor $\phi_j(t)$ changes when the particle moves along the direction of the scattering vector as we mentioned before 2.2.

According to the above dynamic light scattering theory, when a plane wave is scattered by Brownian particles, the electric wave has both amplitude fluctuations and phase fluctuations. A single-mode coherent field experiencing random changes in both amplitude and Schawlow-Townes phase jumps the fluctuating properties seen in light scattered by a suspension of microspheres or rotating ground glass. This field can be presented through a straightforward phenomenological model, inspired by radio communication's amplitude modulation formalism, where the coherent amplitude experiences random modulation. More comprehensive models might describe amplitude fluctuations resulting from numerous factors, such as cavity vibration, changes in laser gain medium, variations in loss or pump, or from relaxation oscillations. These more detailed models can draw upon the theories developed for modeling the relative intensity noise (RIN) in semiconductor lasers. Our simpler approach captures the essential characteristics of these complex models and provides a clear understanding of how amplitude fluctuations affect the system. At the same time, this approach is easily manageable and provides analytical results. Thus, we are using this example to examine a light source. In this case, the light wave's amplitude (or intensity) is modulated by an external signal with fluctuating frequency, conforming to specific correlation relationships

$$\langle f_{mod}(t)\rangle = 0, \quad \langle f_{mod}(t_2) f_{mod}(t_1)\rangle = \frac{1}{2\tau_{int}\sigma(t_2 - t_1)} \tag{4.12}$$

Here, τ_{int} represents the correlation time of intensity fluctuations. Considering a single wave's statistical average, it can be interpreted as the average of the amplitude and phase jumps over time. For the sake of simplicity, we might assume that amplitude and phase oscillations do not affect each other and that the depth of the amplitude modulation is substantial. Thus, we can ignore the unmodulated part of the carrier wave. In this case, the first-order correlation function can be written as

$$g^{(1)}(\tau) = e^{i\omega\tau} e^{-|\tau|/(4\tau_{int})} e^{-|\tau|/(\tau_c)} \tag{4.13}$$

Where the correlation time of the field τ_c includes both phase and amplitude modulations,

$$\frac{1}{\tau_c} = \frac{1}{\tau_\phi} + \frac{1}{4\tau_{int}} \tag{4.14}$$

Thus, it is possible to compute the second-order correlation function for a wave undergoing amplitude variations, as follows

$$g^{(2)}_{amp}(\tau) = 1 + \frac{1}{2}e^{-|\tau|/\tau_{int}} \tag{4.15}$$

This is kind of like the second-order correlation function in a chaotic field, where the photons tend to clump together when $\tau = 0$. But unlike in the chaotic field, this peak has no relation with the first-order correlation function $g^{(1)}(\tau)$ or the field's range of different frequencies. Following the rules of the standard second-order coherence function, it can compute the interference parts in $g^{(2X)}$ as follows

$$g^{(2)}(\sigma, \tau, \sigma + \tau, 0) = (1 + \frac{1}{2}e^{M/\tau_{int}})e^{-2m/\tau_c} \tag{4.16}$$

Where M equals the larger value between $|\sigma|$ and $|\tau|$ the absolute value of time delay σ or the time difference τ. Therefore, $g^{(2X)}$ can be represented as follows.

$$\begin{aligned} g^{(2)}_{amp}(\tau, \sigma) = 1 + [\frac{1}{4}e^{-\tau/\tau_i nt} - \frac{1}{2}(1 + \frac{1}{2}e^{M/\tau_{int}})e^{-2m/\tau_c}] \\ + \frac{1}{8}e^{-|d/c+\tau|/\tau_{int}} + \frac{1}{8}e^{-|d/c-\tau|/\tau_{int}} \end{aligned} \tag{4.17}$$

To simplify, the factors influencing advancements in the central region of the curve around $\tau \approx 0$ are contained within square brackets[...].

The second-order interferometric intensity cross-correlation function for a coherent field undergoing amplitude alterations at fluctuating frequencies displays a coherent state characteristic. This is shown as a dip at roughly $t \approx 0$, decreased to $g^{(2X)}_{amp}(0, \sigma) = 0.75$, and demonstrating a spread of $2/\tau_c$. However, unlike a steady coherent wave, variations in amplitude cause the central component of $g^{(2X)}_{amp}(\tau, \sigma)$ to result in a wide peak with a width of $1/\tau_{int}$. In this case, a noticeable decrease in

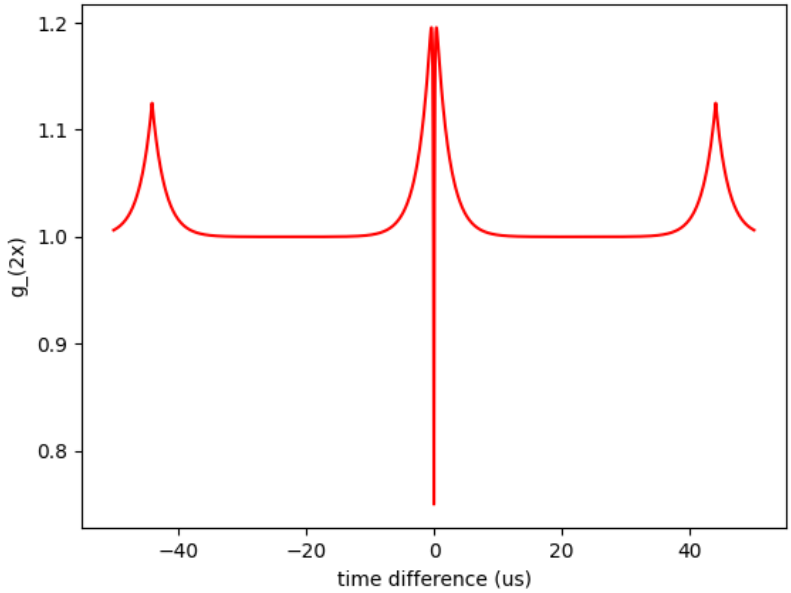

Figure 4.7: Interferometric photon correlation function $g^{(2X)}$ for a stable coherence light source with amplitude modulation Simulation with long time delay $\sigma = 4\tau_c$.

coherence occurs when $2/\tau_c < 1/\tau_{int}$. Therefore, the central segment of $g^{(2X)}_{amp}(\tau, \sigma)$ determines the coherence time of the laser and the correlation time of amplitude fluctuations. At points away from the center $g^{(2X)}_{amp}(\tau, \sigma)$ exhibits two peaks located at $\tau = \pm\sigma$, mirroring two offset versions of the autocorrelation function, which is similarly observed in the chaotic field. According to the equation 4.17, When there is a long time delay between the two beams of light that is nearly five times the coherence time of the scattered light, $g^{(2X)}$ is as shown in the figure 4.7.

The DLS measurement method was combined with the interferometric photon correlation measurement of the laser light to finally form the setup diagram 4.9. According to the DLS measurement method introduced in section 3, the following points are used to reduce the influence of multiple scattering: use two parallel polarizers placed before the light propagates to the cuvette and before collecting scattered light to fibre, use a lens to bring the observation direction and laser irradiation direction close to the surface of the cuvette to reduce the pathway of light, and add solvent to dilute the solution in the cuvette. The rest part of the setup is similar to the cross correlation measurement of laser light.

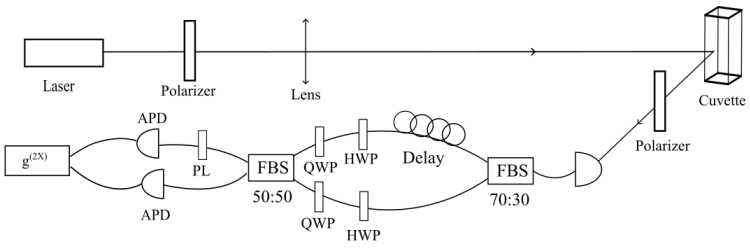

Figure 4.8: Theoretical setup for measuring interferometric photon correlation of scattering light by Brownian particle combining with dynamic light scattering measurement

In the experiment, we still used the laser diode with a central wavelength of around 658nm to generate a stable coherent light source. In this case, we increased the current of the laser diode to 62mA to generate a stronger power of laser light so that counts from scattered light could be detected by APDs. The focal length of the lens is 10cm to focus the beams to the surface of the cuvette. Silica colloid diluted by distilled water as a solvent with 20nm diameter of Brownian particles was selected as the microsphere suspension solution. As we mentioned in section 4, During the experiment, we used an oven controller to heat the solution temperature to approximately 70 Celsius and selected a scattering angle of approximately 150 degrees to collect the intensity of scattered light to reduce the coherence time of scattered light. Finally, through the experimental method of the normal second-order coherence function of scattered light in section 3, we found that the coherence time obtained by fitting in Gaussian distribution is about 11us.

After collecting light into the fiber, the scattering light is split into two beams through a 70:30 fiber beam splitter, and one of the beams is delayed through a 400m fiber, which means $2\mu s$ time delay between two beams, to form an asymmetric MachZehnder interferometer. Then the two beams are interfered through a 50:50 fiber beamsplitter. A half-wave plate and a quarter-wave plate composed of a fiber polarization controller are used to adjust the polarization directions of the two light beams to the same so as to achieve the interference of two beams. Finally, two actively quenched silicon single photon avalanche photo diodes (APD) were used to collect photonevents to observe interferometric photon correlations in the second-order coherence function. Due to the coherence time of scattering light by

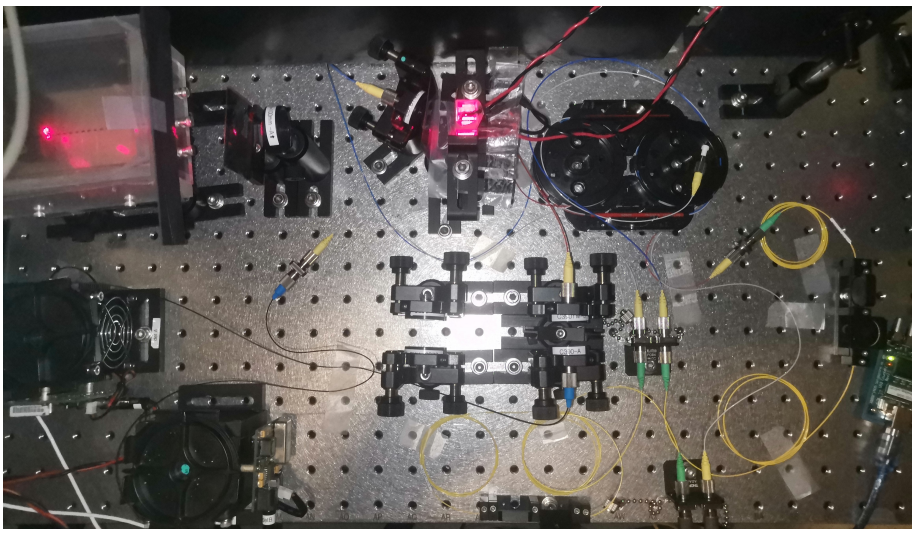

Figure 4.9: Actual setup for measuring interferometric photon correlation of scattered light by silica colloid in lab

microsphere suspension is on the order of microseconds, the interval of each time bin would be larger to increased the time scale of measurement. In this instance, the identified photoevents were timestamped at a 10 ns resolution for an integration period T. The illustration representing the actual setup used in the lab is provided in figure 4.9.

Since the minimum coherence time of scattered light is $11\mu s$ by changing the parameters of solution, the time delay between the two beams passing through the 400m fibre in the experiment is $2\mu s$. In other words, the photon bunching caused by the amplitude fluctuation cannot be well separated from the two peak values of the coherence time of scattered light in this case. Therefore, according to the experimental results as shown in the figure 4.11, we currently cannot see the clear separation of the two peaks from each other. In this case, we can only see an obvious dip near the zero time difference which is apparently different from the second-order coherence function $g^{(2X)}$ with dynamic light scattering method only.

If we zoom in on the cross $g^{(2X)}$ plot at the zero time difference, we can see that there is a clear dip here. A 10m NIM cable was used in the experiment to advance the second-order coherence function plot by approximately 40ns during calculation. It can be seen that there are still three points before the lowest value of dip and eventually drop to the lowest point. Taking the highest and lowest points of the

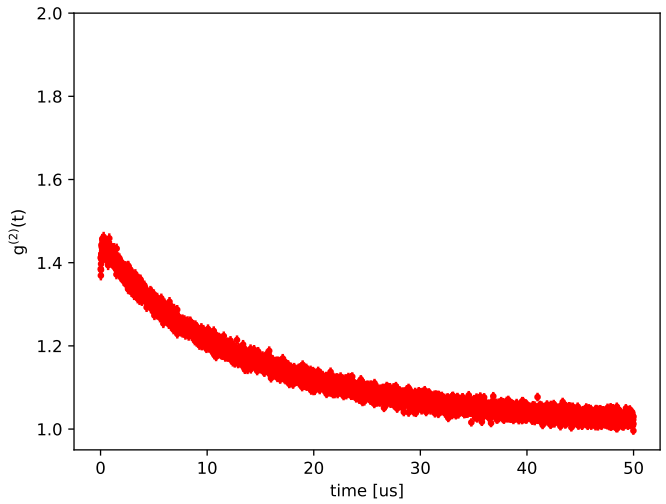

Figure 4.10: Interferometric photon correlations $g^{(2X)}$ for 62mA current laser diode scattered by 20nm silica colloid

dip at the center position, we can get the amplitude of the dip to be approximately 0.088202 which is consistent with the amplitude of the dip measured in the cross $g^{(2x)}$ of the laser diode. This proves the correctness of our experiment and the possibility of using this method to separate amplitude fluctuations and the central coherence of the light source. Since the amplitude fluctuations and the coherence of light cannot be completely distinguished, we currently cannot obtain the coherence time of the amplitude fluctuations and the coherence time of the phase fluctuations by fitting the two patterns respectively, so as to make predictions about the coherence properties of the light scattered by Brownian particles or qualitative analysis of amplitude and phase fluctuations. So our next experiment is to separate the two peaks by using longer optical fibers to increase the time delay or once again reducing the coherence time of the scattered light.

4.4 Summary

This chapter introduces the principle of interferometric photon correlation measurement in laser and scattered light by Brownian particles, as well as the experimental implementation and analysis of the results. Since the laser is a stable coherent light source and its electric field only has phase fluctuations, a dip will appear at

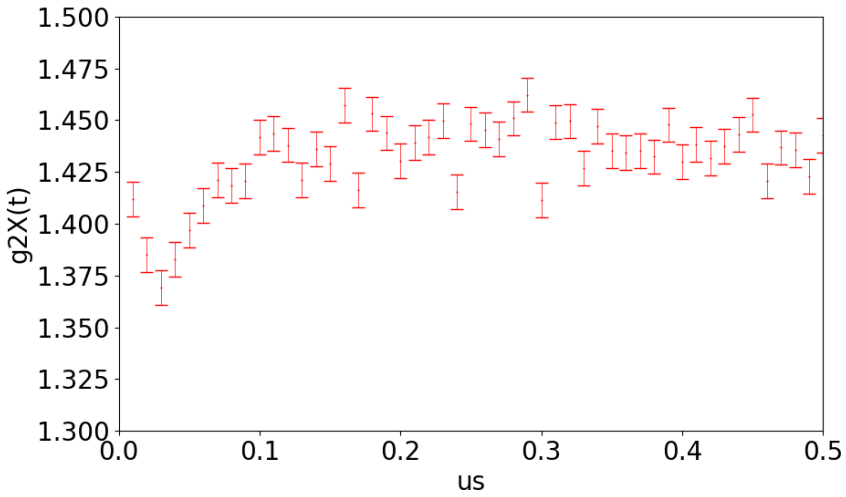

Figure 4.11: Zoom in the central part of $g^{(2X)}$ measuring in experiment.

the center of the 0 time difference of the cross $g^{(2X)}$ image generated by the path difference between the two beams, and the width of this dip is depended on the phase jump of the laser. In the experiment, we used a laser diode to generate a stable laser light source and saw this dip clearly through this experiment. For scattered light, there are both amplitude fluctuations and phase fluctuations. These two fluctuations can be separated and analyzed respectively through cross-correlation measurement. Due to the need for a longer time delay or shorter coherence time, clear phenomena cannot currently be seen in the experiment. We will present specific ideas for implementing the experiment in the next section of the discussion.

Chapter 5

Conclusion and Discussion

As a conclusion, this thesis focuses on the study of the coherent properties of laser light scattered by Brownian particles. The experiment focuses on measuring the classical second-order coherence function $g^{(2)}$ of coherent light and the interferometric photon-correlation second-order coherence function $g^{(2X)}$.

By measuring the classical second-order coherence function of scattered light, we verified the accuracy of the basic formulas related to the diffusion coefficient and scattering vector in the dynamic light scattering theory and studied changing parameters such as experimental environment and solution conditions to reduce the coherence time of scattered light to the minimum. Therefore, it can help us fund the foundation for the measurement of the interferometric second-order coherence function.

In the interferometric photon correlation measurement experiment, we use the stable coherent light source laser diode as the basic measurement object. A clear dip can be seen in the experimental conclusion, which proves the correctness of the $g^{(2X)}$ theory and the feasibility of the experiment. It also provides a stable coherent laser light source for scattered light. In the experiment of measuring $g^{(2X)}$ of scattered light, the current result cannot separate the amplitude fluctuations from the center because the time delay of the two beams is smaller than the coherence time of the scattered light. Therefore, a clear $g^{(2X)}$ plot of scattered light cannot be seen under these conditions. But we still can observe a clear dip in the center, which does not exist in the classical second-order coherence function and is consistent with the assumptions of interferometric theory.

To further analyze the phase fluctuations and amplitude fluctuations of scattered light and distinguish thermal light and pseudothermal light through these

experiments, we need to further improve the experimental conditions to achieve the separation from the central part of the $g^{(2X)}$ plot. In the experiment, how to improve the experimental conditions to achieve this effect can start from the following points: 1. Increase the time delay of the two beams of light. In the experiment, we used 400m optical fiber to achieve the time delay of the two beams of light, which can only produce a time delay of 2us. For clearer phenomena, we need to consider longer optical fibers. 2. Reduce the coherence time of scattered light. In the experiment, a 20nm diameter silica colloid with distilled water as the solvent was used and heated to 70 degrees Celsius as a suspension. It was irradiated with a 658nm laser and the scattered angle was about 150 degrees. Under this condition the coherence time is 11us. By further adjusting the experimental parameters to reduce the coherence time, the peaks of the amplitude fluctuations can be separated.

References

[1]B. J. Berne and R. Pecora, "Dynamic light scattering: with applications to chemistry, biology, and physics", (Courier Corporation, 2000).

[2]W. Martienssen and E. Spiller, "Coherence and Fluctuations in Light Beams", American Journal of Physics **32**, 919–926 (1964).

[3]C. W. Chou, S. V. Polyakov, A. Kuzmich, and H. J. Kimble, "Single-photon generation from stored excitation in an atomic ensemble", Phys. Rev. Lett. **92**, 213601 (2004).

[4]D. Ferreira, R. Bachelard, W. Guerin, R. Kaiser, and M. Fouché, "Connecting field and intensity correlations: the siegert relation and how to test it", American Journal of Physics **88**, 831–837 (2020).

[5]G. Maret and P. Wolf, "Multiple light scattering from disordered media. the effect of brownian motion of scatterers", Zeitschrift für Physik B Condensed Matter **65**, 409–413 (1987).

[6]P.-A. Lemieux and D. Durian, "Investigating non-gaussian scattering processes by using nth-order intensity correlation functions", JOSA A **16**, 1651–1664 (1999).

[7]R. H. Brown and R. Q. Twiss, "Correlation between photons in two coherent beams of light", Current Science **66**, 945–947 (1994).

[8]R. Q. Twiss, A. G. Little, and R. H. Brown, "Correlation between photons, in coherent beams of light, detected by a coincidence counting technique", Nature **180**, 324–326 (1957).

[9]A. Lebreton, I. Abram, R. Braive, I. Sagnes, I. Robert-Philip, and A. Beveratos, "Theory of interferometric photon-correlation measurements: differentiating coherent from chaotic light", Physical Review A **88**, 013801 (2013).

[10]A. Siegert and M. I. of Technology. Radiation Laboratory, "On the fluctuations in signals returned by many independently moving scatterers", Report (Massachusetts Institute of Technology. Radiation Laboratory) (Radiation Laboratory, Massachusetts Institute of Technology, 1943).

[11]R. Pecora, "Dynamic light scattering: applications of photon correlation spectroscopy", in (2011).

[12]R. Ragheb and U. Nobbmann, "Multiple scattering effects on intercept, size, polydispersity index, and intensity for parallel (vv) and perpendicular (vh) polarization detection in photon correlation spectroscopy", Scientific Reports **10**, 10.1038/s41598-020-78872-4 (2020).

[13]R. J. Glauber, "The quantum theory of optical coherence", Physical Review **130**, 2529 (1963).

[14]M. Alexander and D. G. Dalgleish, "Dynamic light scattering techniques and their applications in food science", Food Biophysics **1**, 2–13 (2006).

[15]D. Dravins, T. Lagadec, and P. D. Nuñez, "Long-baseline optical intensity interferometry-laboratory demonstration of diffraction-limited imaging", Astronomy & Astrophysics **580**, A99 (2015).

[16]A. Khomyakov, S. Mordanov, and T. Khomyakova, "The experimental data on the density, viscosity, and boiling temperature of the coffee extract", in Iop conference series: earth and environmental science, Vol. 548, 2 (IOP Publishing, 2020), p. 022040.

[17]J. Cooper and R. Dooley, "The international association for the properties of water and steam", Proceedings of the International Association for the Properties of Water and Steam (IAPWS) (1993).

[18]"Viscosity of water", Website, https://wiki.anton-paar.com/en/water/.

[19]A. Lebreton, I. Abram, R. Braive, I. Sagnes, I. Robert-Philip, and A. Beveratos, "Unequivocal differentiation of coherent and chaotic light through interferometric photon correlation measurements", Physical Review Letters **110**, 163603 (2013).

[20]R. J. Glauber, "Coherent and incoherent states of the radiation field", Physical Review **131**, 2766 (1963).

[21]R. Loudon, "The quantum theory of light", (OUP Oxford, 2000).

[22]N. A. Clark, J. H. Lunacek, and G. B. Benedek, "A study of brownian motion using light scattering", Am. J. Phys **38**, 575–585 (1970).